scientific reports

Check for updates

OPEN

Decoding the transmission and subsequent disability risks of rabineurodeficiency syndrome without recuperation

Yasir Ramzan[1,2], Bandar M. Fadhl[3,4], Shafiullah Niazai[5]✉, Aziz Ullah Awan[2] & Kamel Guedri[3]

This study presents a novel approach focused on extensively addressing the dynamics of Rabineurodeficiency Syndrome by developing a mathematical compartmental model without recuperation. The equilibria of the rabies-free and present states are analyzed locally and globally. Real-world data on annual rabies cases are integrated to confirm and enhance the model's accuracy. Likewise, a parameter estimation technique is employed to optimize the model, aiding in calculating the basic reproduction number. Sensitivity analysis examines the impact of critical parameters on transmission dynamics, providing a deeper understanding of the determining factors influencing disease spread. Visual representations of the relationship between essential parameters and the reproduction number offer valuable insights into factors influencing disease control. Advancing the understanding of Rabineurodeficiency Syndrome dynamics, the inclusive control actions to mitigate infectious diseases are evaluated, emphasizing the importance of accounting for individuals with disabilities.

Keywords Rabineurodeficiency Syndrome, Mathematical Formulation, Stability Analysis, Parameter Estimation, Sensitivity Analysis, Control Strategies

The Rhabdoviridae lineage exhibits RNA structure recognized by a negative strand orientation under the Mononegavirales taxonomic classification, which is the source of the highly contagious disease rabies caused by the Lyssavirus[1]. The terminology rabies is presumed to have sourced from either the Sanskrit "rabhas" (which means an act of aggression) or the Latin "rabere" (which conveys a state of Wrath). At the same time, in antiquated Greek, it was pointed out to as "lyssa" (Indicating an act of violence)[2]. The first recorded occurrence of rabies can be obtained in the "Zuozhuan" text, marked over the 11th year of Xianggong, detailing interactions with rabies carrying dogs in Lu around 556 B.C., underscoring the presence of rabies for around two and a half millennia[3,4].

Rabies is usually known as a zoonotic disease frequently transmitted to humans by bites of animals. The most important animals are dogs among animals globally[5]. In the rising world, human rabies cases are nearly always spread by rabid dogs[6]. The economically developing nations, notably those in Asia and Africa, like India, exhibit the maximum occurrence of loss of human lives caused by rabies. In these countries, domestic canines endure as the main carriers of the disease[7]. In 1908, Zinke was the first to confirm the first recognized proof that saliva is a substantial spread carrier of rabies virus[8,9].

Despite the convenience of operative vaccines, dog rabies is still responsible for the deaths of a minimum of 59,000 lives annually[10]. China is considered second only to India globally in the number of people killed by rabies annually[11]. In 1993, the WHO recorded 31,223 deaths, with a likely additional 10,000 unreported cases, mainly in China, Bangladesh, and Pakistan. The majority of loss of life occurs in counties where rabies is endemic, and healthcare admittance is limited. Even in the USA, which practices endemic rabies in wildlife, the number of deaths was moderately low, with fewer than three loss of life per 100 million people in 1994, compared to up to 3500 cases per 100 million in India[12]. Less than 1% of all rabies cases worldwide are caused by non-rabies viruses in humans[13].

[1]Department of Mathematics, Shanghai University, 99 Shangda Road, Shanghai 200444, China. [2]Institute of Mathematics, University of the Punjab, Lahore 54590, Pakistan. [3]Mechanical Engineering Department, College of Engineering and Architecture, Umm Al-Qura University, P. O. Box 5555, Makkah 21955, Saudi Arabia. [4]King Salman Center for Disability Research, Riyadh 11614, Saudi Arabia. [5]Department of Mathematics, Education Faculty, Laghman University, Mehterlam City, Laghman 2701, Afghanistan. ✉email: shafiullahniazai@lu.edu.af

Rabies is considered one of the 17 globally ignored tropical diseases. Currently, the world is characterized by three main zones regarding rabies: areas with endemic canine rabies and regions where animal rabies persists. In contrast, canine rabies is managed or eradicated in so-called rabies-free areas. Endemic canine rabies residues are dominant in most countries in the Middle East, Africa, and Asia, exposing inhabitants to dog-mediated and animal rabies risks. The United States, Canada, and Western Europe fall into the second category, where transmission through dogs and other canids like coyotes, jackals, foxes, and wolves has been organized or eliminated[14]. However, wildlife such as bats still carry the danger of rabies spreading in these regions and others. Wide-ranging rabies eradication has been attained only in partial areas, largely due to the topographical separation of many places, such as New Zealand, Hawaii, Bahrain, Japan, and much of Oceania, reflected in rabies-free regions. On the other hand, areas that have never had a confirmed human case of lyssavirus infection nearby are considered rabies-free zones[15].

Rabies induces viral Encephalic inflammation, resulting in the Fatality of approximately 70000 individuals annually on a global scale. Viral Encephalic inflammation is transmitted to humans through the saliva of afflicted animals. Rabies, as an affliction, holds historic signification, with cases tracing back four thousand years ago. All through most of human presence, a bite from a rabies-infected animal was widely fatal. In previous times, the populace exhibited such overwhelming anxiety towards rabies that, after being bitten by a potentially rabies-infected critter, numerous individuals would resort to self-inflicted death[16].

Rabies transmits through the saliva of infected animals via bites, replicates in the body before infiltrating the central nervous system, and causes disabilities in behavior and brain function. The virus then migrates to the salivary glands, shed through saliva, facilitating further transmission as depicted in Figure (1). Initial symptoms include pain and numbness near the bite, often delayed for 20 to 50 days but can vary widely. Facial or neck bites may prompt quicker symptom onset. Fever, headaches, malaise, restlessness, and agitation follow, progressing to hallucinations, insomnia, and increased saliva production. Muscle spasms in the throat hinder swallowing, speaking, and breathing, causing disabilities in these functions, with pain even with gentle stimuli. Rabies-induced aversion to water, or hydrophobia, is common. As the disease worsens, it causes "Rabineurodeficiency Syndrome," which is characterized by increasing symptoms including anxiety, agitation, and disorientation. This condition finally leads to unconsciousness, exhaustion, and death[17,18]. The neurological impairments brought on by a rabies infection are known as "Rabineurodeficiency Syndrome".

The backgrounds of modern and current mathematical epidemiology, which rely on compartment models, were established and utilized in the early 20th century[19–21]. The use of mathematical modeling[22,23] has become significantly crucial in the field of epidemiology. It benefits in comprehending observed epidemiological configurations, managing diseases and stability, and gaining insights into the mechanisms that drive disease spread, potentially and possibly suggesting effective control policies. One can assess sensitivity and compare different states and scenarios through model formulation, simulation, and parameter estimation.

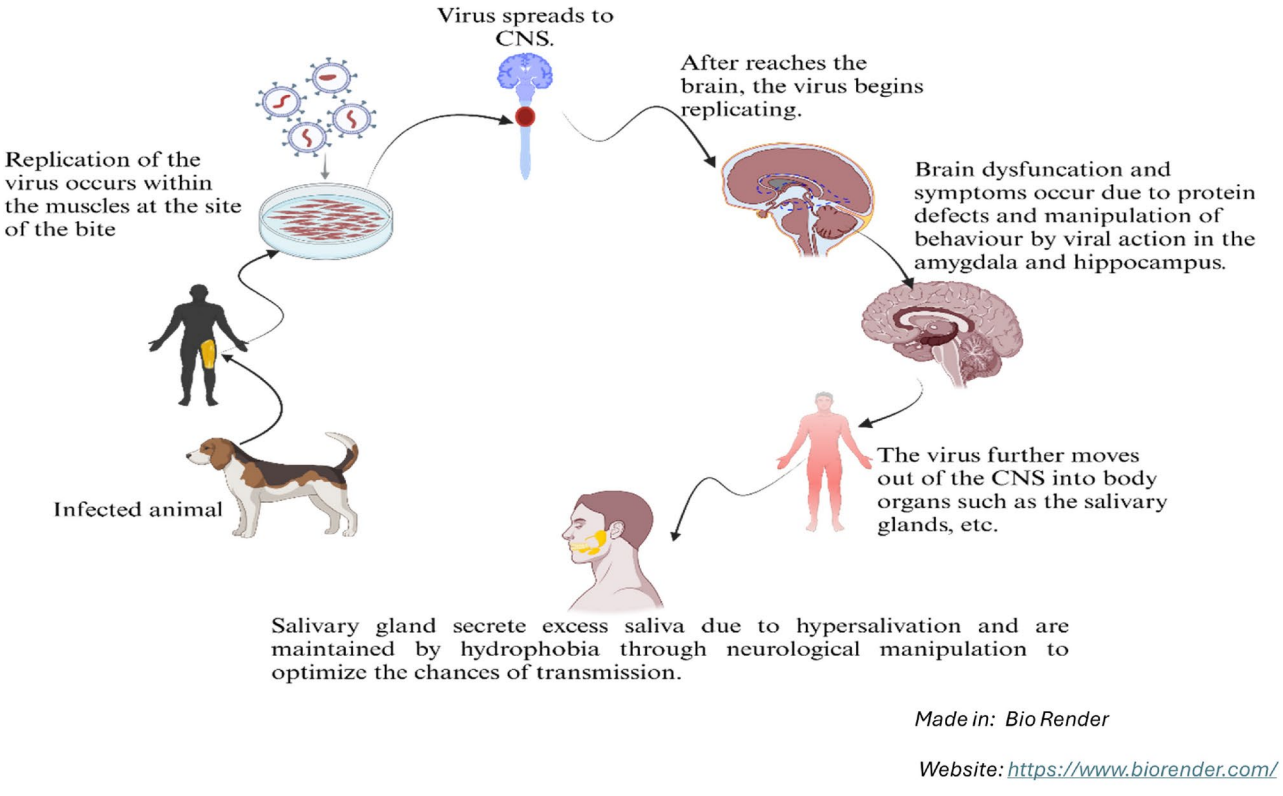

Fig. 1. Rabies transmission cycle.

The study of rabies has a rich history knotted and related with mathematical models, reflecting the broader development of mathematical methods in analyzing and studying infectious disease ecology over the past 30 years[24]. Several models have been employed to explore various sides of rabies in wild animal populations or inhabitants, such as[3,25]. Guedri *et al.*[3] developed a model, studied the dynamics of rabies with healing, and devised intervention strategies to reduce the virus transmission. Wen Gao Lu *et al.*[26] established a mathematical framework to study how the canine rabies virus infects people and suggested some approaches to control virus spread. However, delivering an inclusive portrayal of their findings is still necessary. Further, Zainab et al.[27] worked on the fractional ordered single-population model for rabies transmission, but in this study, the zoonotic (multi-population) model is utilized, which makes it different from existing literature.

The mathematical model developed analyzes different classes without recovery, providing the basis for the novelty of this study. The positive invariance of the system is verified, and the local and global stabilities of rabies-free and endemic states are analyzed to check stability. Utilizing real-world data, a parameter estimation technique is employed to calculate the reproduction number, which helps estimate the ratio at which the disease spreads from infectious to susceptible individuals. After sensitivity analysis, various control parameters are utilized in the model to simulate the specific properties of different interpolation approaches. Graph analysis shows how these control parameters influence the spread of rabies, providing insights into effective disease control and management strategies.

Mathematical framework

The mathematical model considered is an improved version of the framework outlined in[28], which incorporates and integrates six distinct classes to capture the complex and difficult dynamics of rabies within two species, humans and animals. The total host population is distributed into four sub-compartments susceptible compartment $S_h(t)$, Exposed $E_h(t)$, asymptotic $A_h(t)$ and infectious $I_h(t)$. In contrast, the population of animals is apportioned into susceptible $S_v(t)$ and infected animals $I_v(t)$. The spontaneous medium of virus spread among humans and animals arises through the bite of rabid animals. Further explanation of the model can be seen in the flow diagram Figure (2).

The individuals are added into susceptible humans S_h directly by the birth rate Λ, while transmission resulting from infectious animal-human interactions with susceptible hosts occurs at different rates marked as α_1 and α_2. It is assumed that some individuals may transition directly to the infectious category as a consequence of immediate or acute exposure, while others may initially enter the exposed category to signify a latent phase prior to developing infectiousness. The natural mortality of the human population is denoted by μ_h. The compartment E_h represents exposed individuals in the early stage of potential infection, awaiting symptom manifestation. They undergo infection due to animal-human interactions at α_1 and transition to infectious at σ . The compartment A_h denotes asymptomatic humans, where individuals spread the disease without showing symptoms, with the rate Ω governing the transition to asymptomatic or infected states, where susceptible individuals directly transition into infectious with the rate α_2.

The compartment S_v represents susceptible animals, which are influenced by the birth rate Ψ. Transmission among animals occurs with rate β_1 and between human-animal with rate β_2, where animals natural mortality is μ_v. The interpretive expression for the model is described in a flow diagram, and here is the mathematical framework of the compartmental model.

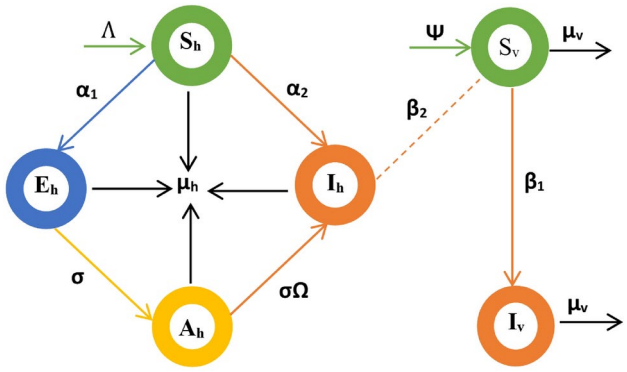

Fig. 2. Flow diagram of compartmental model.

$$\begin{aligned}
\frac{dS_h}{dt} &= \Lambda - (\alpha_1 + \alpha_2) S_h I_v - \mu_h S_h, \\
\frac{dE_h}{dt} &= \alpha_1 S_h I_v - (\sigma + \mu_h) E_h, \\
\frac{dA_h}{dt} &= \sigma(1-\Omega) E_h - \mu_h A_h, \\
\frac{dI_h}{dt} &= \sigma \Omega E_h + \alpha_2 S_h I_v - \mu_h I_h, \\
\frac{dS_v}{dt} &= \Psi - \beta_1 S_v I_v - \beta_2 S_v I_h - \mu_v S_v, \\
\frac{dI_v}{dt} &= \beta_1 S_v I_v + \beta_2 S_v I_h - \mu_v I_v.
\end{aligned} \tag{1}$$

These equations abridge and summarize the dynamics of rabies transmission and progression within both human and animal populations, providing a basic foundation for studying the effectiveness of different control measures and interventions in justifying the spread of the disease. To evaluate the development and qualitative properties of the model, it is imperative to analyze stability, encompassing examination of equilibrium points and sensitivity to parameter variations.

Positively invariant region

To verify the positive invariance of the rabies model, the study begins by defining two populations N_h and N_v, representing the total human and animal populations, respectively, within the system. These populations encapsulate the sum of individuals across various compartments, including susceptible, exposed, asymptomatic, and infected individuals for hosts, respectively, as well as for animals susceptible and infected animals, respectively. The initial conditions needed to simulate Eq. (1) are as follows.

$$S_h(0) \geq 0, \quad E_h(0) \geq 0, \quad A_h(0) \geq 0, \quad I_h(0) \geq 0, \quad S_v(0) \geq 0, \quad I_v(0) \geq 0.$$

The expression $N_h = S_h + E_h + A_h + I_h$ elucidates the entire human population, including individuals at different disease stages, where $N_v = S_v + I_v$ signifies the animal population, with susceptible and infected stages. To ensure the entire population $N_h(t)$ at non negative levels and it remains bounded for all $t > 0$, it is necessary to check that:

$$\begin{aligned}
\frac{dN_h}{dt} &= \Lambda - \mu_h N_h, \\
\frac{dN_v}{dt} &= \Psi - \mu_v N_v.
\end{aligned}$$

Using suitable integration, finally, determine the feasible region for the model 1).

$$\omega = \left\{ (S_h, E_h, A_h, I_h, S_v, I_v) \in \mathbb{R}^6_+ \quad | \quad S_h + E_h + A_h + I_h \leq \frac{\Lambda}{\mu_h}, \quad S_v + I_v \leq \frac{\Psi}{\mu_v} \right\}. \tag{2}$$

The set ω is well defined as the region in the population space where the total number of individuals in each compartment remains below certain thresholds determined by humans' and animals' birth and death rates. The positively invariant solution specifies that within the defined area ω, the dynamics of the rabies disease model lead to a steady and stable state where the total number of individuals in each compartment does not exceed maintainable levels determined by birth and death rates. This steady and stable state is desirable as it suggests that the disease does not lead to uncontrolled population growth, and the system maintains steadiness and stability between births, deaths, and disease transmission.

Rabies free equilibrium

The rabies-free equilibrium in the model represents a state without any infected individuals, indicating the cessation of transmission dynamics. All infected compartments are reset to zero to reach this equilibrium. Its existence suggests that the disease may be completely eradicated, which denotes stability and the lack of recent infections. A rabies free equilibrium point e_0 in model (1) can be articulated as:

$$e_0 = (S_h^0, E_h^0, A_h^0, I_h^0, S_v^0, I_v^0) = \left(\frac{\Lambda}{\mu_h}, 0, 0, 0, \frac{\Psi}{\mu_v}, 0 \right). \tag{3}$$

Basic reproduction number

The average number of secondary infections one sick person causes in a susceptible society is signified by the basic reproduction number (R_0). The next generation matrix approach[29] is utilized to determine R_0 mathematically for the rabies model (1).

$$\hat{U} = \left[\frac{\partial(\hat{U}_i(e_0))}{\partial(x_j)} \right] and \quad \hat{W} = \left[\frac{\partial(\hat{W}_i(e_0))}{\partial(x_j)} \right],$$

Whereas $\hat{W}_i$ indicates the rate of transmission from one compartment to another, $\hat{U}_i$ depicts the secondary infections brought on by a single person in one compartment to another. The infected compartment $x_j = (E_h, A_h, I_h, I_v)$ yields:

$$\hat{U} = \begin{bmatrix} 0 & 0 & 0 & \alpha_1 \frac{\Lambda}{\mu_h} \\ 0 & 0 & 0 & 0 \\ 0 & 0 & 0 & \alpha_2 \frac{\Lambda}{\mu_h} \\ 0 & 0 & \beta_2 \frac{\Psi}{\mu_v} & \beta_1 \frac{\Psi}{\mu_v} \end{bmatrix}, \quad \hat{W} = \begin{bmatrix} (\sigma + \mu_h) & 0 & 0 & 0 \\ -\sigma(1-\Omega) & \mu_h & 0 & 0 \\ -\sigma\Omega & 0 & \mu_h & 0 \\ 0 & 0 & 0 & \mu_v \end{bmatrix},$$

then

$$\hat{U}\hat{W}^{-1} = \begin{bmatrix} 0 & 0 & 0 & \Lambda \frac{\alpha_1}{\mu_h \mu_v} \\ 0 & 0 & 0 & 0 \\ 0 & 0 & 0 & \Lambda \frac{\alpha_2}{\mu_h \mu_v} \\ \Psi\Omega\sigma \frac{\beta_2}{\mu_v(\mu_h^2 + \sigma\mu_h)} & 0 & \Psi \frac{\beta_2}{\mu_h \mu_v} & \Psi \frac{\beta_1}{\mu_v^2} \end{bmatrix}.$$

R_0 is the maximal eigen value of $\hat{U}\hat{W}^{-1}$.

$$R_0 = \frac{1}{2\mu_h \mu_v^2} \left(\sqrt{\frac{1}{\sigma + \mu_h} \left(\Psi^2 \beta_1^2 \mu_h^3 + \Psi^2 \sigma \beta_1^2 \mu_h^2 + 4\Psi\Lambda\beta_2 \mu_v^2 (\sigma\alpha_2 + \alpha_2\mu_h + \Omega\sigma\alpha_1) \right)} + \Psi\beta_1\mu_h \right). \quad (4)$$

Parameter fitting and estimation

Accurate mathematical models of natural biological systems rely on precise parameter fitting using differential equations. This process ensures models closely match observed data and aids in predicting biological phenomena. In infectious disease modeling, parameter fitting optimizes parameters for accurate predictions, informs public health interventions, and enables evidence-based decision-making and epidemic forecasting.

The parameters are fitted and estimated by examining the yearly reports of rabies occurrences in China as documented in the Table (1). The evaluation of calibrated parameter values is detailed in Table (2), which is based on real rabies case data. These values of parameters are assessed concerning the average human lifespan $1996 - 2020$ stands at 73.64 years according to available information[35]. Figure (3) depicts a tally between the observed and estimated numbers of confirmed rabies cases. The line represents the estimated cases, while the scatter plot depicts the actual occurrences of rabies.

The estimated reproduction number lies between [0.0405409, 3.75046]. It is calculated by incorporating estimated parameter values provided in Table (2) and the result after applying the next-generation matrix method.

Theorem 1 *If $R_0 < 1$, then the rabies-free equilibrium of model (1) attains local asymptotic stability within the positive invariant set ω.*

Proof Analyzing the Jacobian matrix's eigenvalues at point (3) is necessary to study the Rabies Free Equilibrium (RFE) and gain an understanding of the system's local stability around this equilibrium[30]. Understanding the behavior of the disease in the absence of the virus requires an analysis of the short-term dynamics of the Rabies virus, which becomes feasible by this evaluation.

$$J^0 = \begin{pmatrix} -\mu_h & 0 & 0 & 0 & 0 & -(\alpha_1 + \alpha_2)\frac{\Lambda}{\mu_h} \\ 0 & -(\sigma + \mu_h) & 0 & 0 & 0 & \alpha_1 \frac{\Lambda}{\mu_h} \\ 0 & \sigma(1-\Omega) & -\mu_h & 0 & 0 & 0 \\ 0 & \sigma\Omega & 0 & -\mu_h & 0 & \alpha_2 \frac{\Lambda}{\mu_h} \\ 0 & 0 & 0 & -\beta_2 \frac{\Psi}{\mu_v} & -\mu_v & -\beta_1 \frac{\Psi}{\mu_v} \\ 0 & 0 & 0 & \beta_2 \frac{\Psi}{\mu_v} & 0 & \beta_1 \frac{\Psi}{\mu_v} - \mu_v \end{pmatrix}.$$

The characteristic equation of this matrix is given as $det(J^0 - \lambda I)$. Expanding this determinant into a characteristic equation, the resulting equation is as follows:

$$(-\lambda - \mu_h)(-\lambda - \mu_v)(-\lambda - \mu_h)(\lambda^3 + m_1\lambda^2 + m_2\lambda + m_3) = 0,$$

where

$$m_1 = \left(\sigma + 2\mu_h + \mu_v - \Psi \frac{\beta_1}{\mu_v} \right) = 1.011 > 0,$$

$$m_2 = \left(\mu_h(\sigma + \mu_h) + \left(\mu_v - \Psi \frac{\beta_1}{\mu_v} \right)(\sigma + 2\mu_h) - \Psi\Lambda\alpha_2 \frac{\beta_2}{\mu_h \mu_v} \right) = 0.114 > 0,$$

$$m_3 = \left(\mu_h(\sigma + \mu_h) \left(\mu_v - \Psi \frac{\beta_1}{\mu_v} \right) + \Psi \frac{\beta_2}{\mu_v} \left(\Lambda\alpha_2 - \Omega\sigma\Lambda \frac{\alpha_1}{\mu_h} \right) - \Psi\Lambda\alpha_2 \frac{\beta_2}{\mu_h \mu_v}(\sigma + 2\mu_h) \right) = 0.001 > 0,$$

when

$$R_0 = 0.0685 < 1.$$

It's obvious that the eigenvalues μ_h and μ_v are negative. Three eigenvalues remain, which are solutions to a certain equation. Extensive computations reveal that these roots are negative if and only if $R_0 < 1$. The necessary and sufficient conditions for local asymptotic stability are established by the Routh Hurwitz criteria as described in[31], so that for $i = 1, 2, 3$, $m_1 m_2 > m_3$ and $m_i > 0$. □
The local asymptotic stability of the rabies-free equilibrium in the model (1) is addressed by Theorem 1, holding significance for rabies virus control and eradication efforts. If the condition $R_0 < 1$ holds, each infected individual transmits less than one secondary infection on average, leading to a decline in disease spread. Understanding long-term dynamics and evaluating control measures against rabies hinge on global stability, a pivotal factor. This is accomplished by utilizing Castillo-Chavez conditions[32], which offers valuable insights into system behavior and the effectiveness of control strategies.

Theorem 2 *If $R_0 < 1$, then the rabies-free equilibrium of model (1) attains global asymptotic stability within the positive invariant set ω.*

Proof The global stability can be analyzed by incorporating Castillo-Chavez conditions outlined in[32]. The state variables utilized in model (1) are $P = (S_h, S_v)$ and $Q = (E_h, A_h, I_h, I_v)$. The model (1) can be written as:

$$\begin{aligned}\frac{dS_h}{dt} &= \Lambda - \mu_h S_h \\ \frac{dS_v}{dt} &= \Psi - \mu_v S_v\end{aligned}$$

solving the system at the RFE point yields

$$\begin{aligned}S_h &= \frac{\Lambda}{\mu_h} - \left(\frac{\Lambda}{\mu_h} - S_h(0)\right) e^{-\mu_h t} \\ S_v &= \frac{\Psi}{\mu_v} - \left(\frac{\Psi}{\mu_v} - S_v(0)\right) e^{-\mu_v t}\end{aligned}$$

when $t \to \infty$, $S_h(t) \to \frac{\Lambda}{\mu_h}$ and $S_v(t) \to \frac{\Psi}{\mu_v}$ irrespective of initial conditions. Thus, the RFE point is globally asymptotically stable. Next, we have

$$V(P,Q) = \begin{pmatrix} \alpha_1 S_h I_v - (\sigma + \mu_h) E_h \\ \sigma(1-\Omega) E_h - \mu_h A_h \\ \sigma\Omega E_h + \alpha_2 S_h I_v - \mu_h I_h \\ \beta_1 S_v I_v + \beta_2 S_v I_h - \mu_v I_v \end{pmatrix}$$

define

$$Z = \begin{pmatrix} -(\sigma+\mu_h) & 0 & 0 & \alpha_1 \frac{\Lambda}{\mu_h} \\ \sigma(1-\Omega) & -\mu_h & 0 & 0 \\ \sigma\Omega & 0 & -\mu_h & \alpha_2 \frac{\Lambda}{\mu_h} \\ 0 & 0 & \beta_2 \frac{\Psi}{\mu_v} & -\mu_v + \beta_1 \frac{\Psi}{\mu_v} \end{pmatrix} \quad \text{and} \quad ZQ = \begin{pmatrix} -(\sigma+\mu_h) E_h + \alpha_1 \frac{\Lambda}{\mu_h} I_v \\ \sigma(1-\Omega) E_h - \mu_h A_h \\ \sigma\Omega E_h - \mu_h I_h + \alpha_2 \frac{\Lambda}{\mu_h} I_v \\ \beta_2 \frac{\Psi}{\mu_v} I_h + \left(\beta_1 \frac{\Psi}{\mu_v} - \mu_v\right) I_v \end{pmatrix}.$$

The off-diagonal entries of the Z matrix are non-negative, so it's M-Matrix. We have

$$\hat{V}(P,Q) = ZQ - V(P,Q) = \begin{pmatrix} \left(\frac{\Lambda}{\mu_h} - S_h\right) \alpha_1 I_v \\ 0 \\ \left(\frac{\Lambda}{\mu_h} - S_h\right) \alpha_2 I_v \\ \beta_1 \left(\frac{\Psi}{\mu_v} - S_v\right) I_v + \beta_2 \left(\frac{\Psi}{\mu_v} - S_v\right) I_h \end{pmatrix}.$$

This completes the proof with the clarity that $\hat{V}(P,Q) \geq 0$, where $0 \leq S_h \leq N_h$,and $0 \leq S_v \leq N_v$. □

Theorem 3 *A unique endemic equilibrium point exists if $R_0 > 1$.*

Proof In compartmental models, endemic equilibrium points represent stable disease occurrence in a population, attained by solving a system of differential equations describing disease dynamics. For rabies, these points indicate a steady state where susceptible, exposed, asymptomatic, and infectious individuals among humans and animals reach equilibrium, signifying disease persistence. Mathematically, this is achieved by setting the derivatives of the model's equations to zero and solving for steady-state compartment values under specific conditions. For $R_0 > 1$, consider $e^* = (S_h^*, E_h^*, A_h^*, I_h^*, S_v^*, I_v^*)$ such that.

$$
\begin{aligned}
S_h^* &= \frac{\Lambda}{((\alpha_1+\alpha_2)I_v^* - \mu_h)},\\
E_h^* &= \frac{\Lambda\alpha_1 I_v^*}{(\sigma+\mu_h)(\alpha_1+\alpha_2)I_v^* - \mu_h)},\\
A_h^* &= \frac{\Lambda\alpha_1\sigma(1-\Omega)I_v^*}{\mu_h((\alpha_1+\alpha_2)I_v^* - \mu_h)(\sigma+\mu_h)},\\
I_h^* &= \frac{(\sigma\Omega\alpha_1\Lambda + \alpha_2\Lambda(\sigma+\mu_h))I_v^*}{\mu_h((\alpha_1+\alpha_2)I_v^* - \mu_h)(\sigma+\mu_h)},\\
S_v^* &= \frac{(BI_v^* + C)\Psi}{(BI_v^* + C)(\beta_1 I_v^* + \mu_v) + \beta_2 A I_v^*},
\end{aligned}
$$

by solving for I_v^* following expression is obtained:

$$AI_v^{*2} + BI_v^* + C = 0,$$

where

$$
\begin{aligned}
A &= \beta_1\mu_h\mu_v\left(\alpha_1+\alpha_2\right)\left(\mu_h+\sigma\right),\\
B &= \mu_h\mu_v\left(\left(\mu_h+\sigma\right)\beta_1\mu_h + \left(\alpha_1+\alpha_2\right)\left(\mu_h+\sigma\right)\mu_v + \Lambda\alpha_2\beta_2\right)\\
&\quad + \left(\alpha_2+\Omega\alpha_1\right)\sigma\Lambda\beta_2\mu_v - \Psi\beta_1\mu_h\left(\alpha_1+\alpha_2\right)\left(\mu_h+\sigma\right),\\
C &= \mu_h^2\mu_v^2\left(\mu_h+\sigma\right) - \Psi\left(\beta_1\mu_h^2\left(\mu_h+\sigma\right) + \Lambda\alpha_2\beta_2\left(\sigma+\mu_h\right) + \Omega\sigma\Lambda\alpha_1\beta_2\right).
\end{aligned}
$$

It isn't easy to check the signs of the coefficients, so proceed with numerical values when $R_0 = 3.782 > 1$

$$A = 8.096\times10^{-23}, \quad B = 2.728\times10^{-13}, \quad C = -1.782\times10^{-07}.$$

The coefficients of I_v^2 and I_v are positive, and constant term changes its sign concerning R_0. There is one sign change, so by Descartes' Rule of Signs, I_v has one positive and one negative root. Hence, a unique Endemic equilibrium occurs. □

Theorem 4 *The model is a globally asymptotically stable state for endemic equilibrium if* $R_0 > 1$.

Proof Considering Lyapunove function:

$$
\begin{aligned}
L = &\frac{\beta_2 S_v^* I_h^*}{(\alpha_1 S_h^* I_v^* + \alpha_2 S_h^* I_v^*)}\left(S_h - S_h^* - S_h^*\ln\frac{S_h}{S_h^*}\right) + \frac{\beta_2 S_v^* I_h^*\sigma\Omega E_h^*}{(\alpha_1 S_h^* I_v^*)(\sigma\Omega E_h^* + \alpha_2 S_h^* I_v^*)}\left(E_h - E_h^* - E_h^*\ln\frac{E_h}{E_h^*}\right)\\
&+ \frac{\beta_2 S_v^* I_h^*}{(\alpha_2 S_h^* I_v^* + \sigma\Omega E_h^*)}\left(I_h - I_h^* - I_h^*\ln\frac{I_h}{I_h^*}\right) + \left(S_v - S_v^* - S_v^*\ln\frac{S_v}{S_v^*}\right) + \left(I_v - I_v^* - I_v^*\ln\frac{I_v}{I_v^*}\right),
\end{aligned}
$$

taking derivative of L with respect to time

$$
\begin{aligned}
L' = &\frac{\beta_2 S_v^* I_h^*}{(\alpha_1 S_h^* I_v^* + \alpha_2 S_h^* I_v^*)}\left(1 - \frac{S_h^*}{S_h}\right)S_h' + \frac{\beta_2 S_v^* I_h^*\sigma\Omega E_h^*}{(\alpha_1 S_h^* I_v^*)(\sigma\Omega E_h^* + \alpha_2 S_h^* I_v^*)}\left(1 - \frac{E_h^*}{E_h}\right)E_h'\\
&+ \frac{\beta_2 S_v^* I_h^*}{(\alpha_2 S_h^* I_v^* + \sigma\Omega E_h^*)}\left(1 - \frac{I_h^*}{I_h}\right)I_h' + \left(1 - \frac{S_v^*}{S_v}\right)S_v' + \left(1 - \frac{I_v^*}{I_v}\right)I_v',
\end{aligned}
$$

substituting the expressions from model (1)

$$
\begin{aligned}
L' = & \frac{\beta_2 S_v^* I_h^*}{(\alpha_1 S_h^* I_v^* + \alpha_2 S_h^* I_v^*)} \left[S_h^* I_v^* \left(1 - \frac{S_h I_v}{S_h^* I_v^*} - \frac{S_h^*}{S_h} + \frac{I_v}{I_v^*} \right) (\alpha_1 + \alpha_2) + \mu_h S_h^* \left(2 - \frac{S_h}{S_h^*} - \frac{S_h^*}{S_h} \right) \right] \\
& + \frac{\beta_2 S_v^* I_h^* \sigma \Omega E_h^*}{(\alpha_1 S_h^* I_v^*)(\sigma \Omega E_h^* + \alpha_2 S_h^* I_v^*)} \alpha_1 S_h^* I_v^* \left(\frac{S_h I_v}{S_h^* I_v^*} - \frac{E_h}{E_h^*} - \frac{E_h^* S_h I_v}{E_h S_h^* I_v^*} + 1 \right) \\
& + \frac{\beta_2 S_v^* I_h^*}{(\alpha_2 S_h^* I_v^* + \sigma \Omega E_h^*)} \left[\sigma \Omega E_h^* \left(\frac{E_h}{E_h^*} - \frac{I_h}{I_h^*} - \frac{I_h^* E_h}{I_h E_h^*} + 1 \right) + \alpha_2 S_h^* I_v^* \left(\frac{S_h I_v}{S_h^* I_v^*} - \frac{I_h}{I_h^*} - \frac{I_h^* S_h I_v}{I_h S_h^* I_v^*} + 1 \right) \right] \\
& + \left[\beta_1 S_v^* I_v^* \left(1 - \frac{I_h S_v}{I_h^* S_v^*} - \frac{I_v^*}{S_v} + \frac{I_h}{I_h^*} \right) + \beta_2 S_v^* I_h^* \left(1 - \frac{S_v}{S_v^*} \frac{I_v}{I_v^*} - \frac{S_v^*}{S_v} + \frac{I_v}{I_v^*} \right) + \mu_v S_v^* \left(2 - \frac{S_v}{S_v^*} - \frac{S_v^*}{S_v} \right) \right] \\
& + \left[\beta_1 S_v^* I_v^* \left(\frac{I_h S_v}{I_h^* S_v^*} - \frac{I_v}{I_v^*} - \frac{I_v^*}{I_v} - \frac{I_v^* I_h S_v}{I_v I_h^* S_v^*} + 1 \right) + \beta_2 S_v^* I_h^* \left(\frac{I_v S_v}{I_v^* S_v^*} - \frac{I_v}{I_v^*} - \frac{S_v}{S_v^*} + 1 \right) \right], \\
L' = & \frac{\beta_2 S_v^* I_h^* \mu_h S_h^*}{(\alpha_1 S_h^* I_v^* + \alpha_2 S_h^* I_v^*)} \left(2 - \frac{S_h}{S_h^*} - \frac{S_h^*}{S_h} \right) + (\mu_v S_v^* + \beta_1 S_v^* I_h^*) \left(2 - \frac{S_v}{S_v^*} - \frac{I_v^*}{I_v} \right) \\
& + \frac{\beta_2 S_v^* I_h^* \sigma \Omega E_h^* \alpha_1 S_h^* I_v^*}{(\alpha_1 S_h^* I_v^*)(\sigma \Omega E_h^* + \alpha_2 S_h^* I_v^*)} \left(5 - \frac{S_h^*}{S_h} - \frac{E_h^* S_h I_v}{E_h S_h^* I_v^*} - \frac{I_v^*}{I_v} - \frac{I_v^* I_h S_v}{I_v I_h^* S_v^*} - \frac{I_h^* E_h}{I_h E_h^*} \right) \\
& + \beta_1 S_h^* I_v^* \left(4 - \frac{I_h^* S_h I_v}{I_h S_h^* I_v^*} - \frac{I_v^* S_v I_h}{I_v S_v^* I_h^*} - \frac{S_h^*}{S_h} - \frac{I_v^*}{I_v} \right),
\end{aligned}
$$

Since the arithmetic mean is always greater than or equal to the geometric mean, it follows that,

$$
\begin{aligned}
& 2 - \frac{S_h}{S_h^*} - \frac{S_h^*}{S_h} \leq 0, \\
& 2 - \frac{S_v}{S_v^*} - \frac{I_v^*}{I_v} \leq 0, \\
& 5 - \frac{S_h^*}{S_h} - \frac{E_h^* S_h I_v}{E_h S_h^* I_v^*} - \frac{I_v^*}{I_v} - \frac{I_v^* I_h S_v}{I_v I_h^* S_v^*} - \frac{I_h^* E_h}{I_h E_h^*} \leq 0, \\
& 4 - \frac{I_h^* S_h I_v}{I_h S_h^* I_v^*} - \frac{I_v^* S_v I_h}{I_v S_v^* I_h^*} - \frac{S_h^*}{S_h} - \frac{I_v^*}{I_v} \leq 0.
\end{aligned}
$$

Hence, it shows that $L' \leq 0$. Its also holds when $S_h = S_h^*$, $E_h = E_h^*$, $A_h = A_h^*$, $I_h = I_h^*$, $S_v = S_v^*$ and $I_v = I_v^*$. Thus, by the LaSalle invariance principle[33], the system is globally asymptotically stable. □

Sensitivity analysis

Sensitivity indices provide a quantitative measure of how variations in model parameters affect the key outcome variable, R_0. Chitnis *et al.*[37] presented a precise method using partial derivatives to compute sensitivity indices. The expression for sensitivity indices, $\frac{\partial R_0}{\partial p} \times \frac{p}{R_0}$, measures and quantifies the effect of individual parameters p on R_0. Sensitivity indices are presented in Table (3) and visualized in Figure (4).

The sensitivity analysis highlights key parameters Λ, Ψ, β_1, β_2 and α_2 in rabies transmission. R_0 directly correlates with these parameters, while mortality rates (μ_h and μ_v) inversely affect R_0. The parameters σ, Ω, and α_1 show lower sensitivity.

Optimization of control strategies

Optimal control theory offers a solid foundation for optimizing processes in these kinds of systems. To improve understanding and effectively modify the dynamics of the system, nine time-dependent control variables y_i , where $i = 1, 2, 3, \ldots, 9$, are presented. These variables are introduced by applying optimal control theory to the model given by Eq. (1). The dynamics of the controlled system are governed by the model (5), which shows how different variables change over time. This approach simplifies the process of examining control optimization solutions for complex systems. The challenges and strategies to mitigate rabies, as depicted in Figure (5) are articulated below:

- With a focus on exposed individuals, the Parameter y_1 denotes determinations to lower the interaction rate between susceptible individuals S_h and infected animals I_v. It entails public awareness campaigns that use AI-powered teaching materials to alter human behavior and prevent interaction with possibly diseased animals.
- With a focus on symptomatic infections, the Parameter y_2 denotes determinations to lower the interaction rate between susceptible individuals S_h and infected animals I_v. This involves utilizing customized drug delivery, applying artificial intelligence for predictive modeling, and building barriers to keep people and animals apart.
- The transition rate from exposed individuals E_h to asymptomatic individual infections A_h is decreasing, as indicated by the parameter y_3. It incorporates delivering immediate immunity post-exposure through targeted nanoparticle vaccines that enhance immune response.
- The parameter y_4 characterizes the process of reducing the incidence of disease transmission from asymptomatic people A_h to symptomatic people I_h. It involves using nanoparticles to deliver antiviral drugs that effectively reduce viral load in asymptomatic carriers, preventing further transmission.

- The parameter y_5 indicates the decrease in the number of persons experiencing symptoms, marked as I_h. This step includes Utilizing nanoparticles to transport antiviral treatments directly to infected neural tissues, enabling effective action across the blood-brain barrier.
- The rate of interaction between susceptible animals S_v and infected animals I_v is decreased by the parameter y_6. Alternative approaches to manage fauna include using diversionary tactics and GPS collars to monitor the movement of domestic and wildlife populations to detect rabies spread.
- Reducing the interaction rate between susceptible animal populations S_v and infected human beings I_h is the target of parameter y_7. Artificial intelligence-driven monitoring systems can place barriers and deterrents to lessen the likelihood that people will come into contact with animals.
- The shifting of susceptible individual animals S_v to different compartments is minimized by the parameter y_8 . The paradigm of disease prevention and management is revolutionized by employing AI-driven approaches in developing vaccines in conjunction with nano-scale delivery systems and concentrating immunization efforts on animal reservoirs.
- The y_9 parameter represents the move taken to lower the I_v number of infected animals. Public health efforts to minimize animal exposure to infectious diseases and vaccine programs that target animal reservoirs.

The controlled model is articulated as:

$$\begin{aligned}
\frac{dS_h}{dt} &= \Lambda - ((1-y_1)\,\alpha_1 + r_1 y_2 \alpha_2) S_h I_v - \mu_h S_h \\
\frac{dE_h}{dt} &= (1-y_1)\,\alpha_1 S_h I_v - (\sigma + \mu_h + r_2 y_3) E_h \\
\frac{dA_h}{dt} &= \sigma(1-\Omega) E_h + r_2 y_3 E_h - (\mu_h + r_3 y_4)\, A_h \\
\frac{dI_h}{dt} &= \sigma \Omega E_h + r_3 y_4 A_h + r_1 y_2 \alpha_2 S_h I_v - (\mu_h + r_4 y_5)\, I_h \\
\frac{dS_v}{dt} &= \Psi - r_5 y_6 \beta_1 S_v I_v - r_6 y_7 \beta_2 S_v I_h - (\mu_v + r_7 y_8)\, S_v \\
\frac{dI_v}{dt} &= r_5 y_6 \beta_1 S_v I_v + r_6 y_7 \beta_2 S_v I_h - (\mu_v + r_8 y_9)\, I_v
\end{aligned} \tag{5}$$

To decrease rabies transmission and minimize the counts of infected animals and humans, the main concern is applying nine specific strategies. The final purpose is to achieve these goals or objectives while certifying that our efforts remain cost-effective and reasonable. For this purpose, an objective function is defined:

$$J(y_i) = \int_0^t \left(D_1 S_h + D_2 E_h + D_3 A_h + D_4 I_h + D_5 S_v + D_6 I_v + \frac{1}{2} \sum_{i=1}^{9} B_i y_i^2(t) \right) dt. \tag{6}$$

Let t represent the final time controls are executed inside the interval $[0, t]$. The constants B_i for $i = 1, 2, \ldots, 9$ and $i = 1, 2, \ldots, 6$ represent the total costs associated with control measures y_i. The main aim is to determine the optimal control from nonuplet $y^* = \{y_i^* \mid i = 1, 2, \ldots, 9\}$ that effectively reduces the overall incurred cost.

$$J(y_i^*) = min\{J(y_i) \mid y_i \in Y,\ i = 1, 2, 3, \ldots, 9\}. \tag{7}$$

A non-empty set is described as:

$$Y = \{y_i : 0 \le y_i(t) \le 1,\ t \in [0, t],\ i = 1, 2, 3, \ldots, 9\}.$$

Pontryagin's ultimate principle simplifies optimizing the control parameters into a problem of optimizing the Hamiltonian function. In[38], this effective transformation has been thoroughly examined, with the Hamiltonian function H defined as follows:

$$H = D_1 S_h + D_2 E_h + D_3 A_h + D_4 I_h + D_5 S_v + D_6 I_v + \frac{1}{2} \sum_{i=1}^{9} B_i y_i^2(t) + \sum_{i=1}^{6} \theta_i X_i. \tag{8}$$

The complementary functions associated with the system (5) are characterized by θ_i, while the expressions governing the state variables described in the control system (5) on the right side of the above ODEs are denoted by X_i such that $i = 1, 2, 3, \ldots, 6$. The following format can be used to express the Hamiltonian function:

$$\begin{aligned}
H =& D_1 S_h + D_2 E_h + D_3 A_h + D_4 I_h + D_5 S_v + D_6 I_v + \frac{1}{2} B_1 y_1^2 + \frac{1}{2} B_2 y_2^2 + \frac{1}{2} B_3 y_3^2 + \frac{1}{2} B_4 y_4^2 + \frac{1}{2} B_5 y_5^2 \\
&+ \frac{1}{2} B_6 y_6^2 + \frac{1}{2} B_7 y_7^2 + \frac{1}{2} B_8 y_8^2 + \frac{1}{2} B_9 y_9^2 + \theta_1 (\Lambda - ((1-y_1)\,\alpha_1 + r_1 y_2 \alpha_2) S_h I_v - \mu_h S_h) \\
&+ \theta_2 \left((1-y_1)\,\alpha_1 S_h I_v - (\sigma + \mu_h + r_2 y_3) E_h \right) + \theta_3 \left(\sigma(1-\Omega) E_h + r_2 y_3 E_h - (\mu_h + r_3 y_4)\, A_h \right) \\
&+ \theta_4 \left(\sigma \Omega E_h + r_3 y_4 A_h + r_1 y_2 \alpha_2 S_h I_v - (\mu_h + r_4 y_5)\, I_h \right) \\
&+ \theta_5 \left(\Psi - r_5 y_6 \beta_1 S_v I_v - r_6 y_7 \beta_2 S_v I_h - (\mu_v + r_7 y_8)\, S_v \right) + \theta_6 \left(r_5 y_6 \beta_1 S_v I_v + r_6 y_7 \beta_2 S_v I_h - (\mu_v + r_8 y_9)\, I_v \right)
\end{aligned}$$

The subsequent theorem summarizes the optimal approach, denoted as y^*, targeted at minimizing the problem (7). Notably, the approach used in this framework is based on the work as presented in[39,40].

Theorem 5 *If factors $y_i^* \in Y$ for $i = 1, 2, 3, \ldots, 9$ satisfy (7) concerning the corresponding system (5), then there occurs always a set of associated functions $\theta_1(t), \theta_2(t), \ldots, \theta_6(t)$ for $i = 1, 2, 3, \ldots, 6$ that satisfy the following system.*

$$\begin{aligned}
\frac{d\theta_1}{dt} &= \theta_1\mu_h - D_1 + \theta_1\alpha_1 I_v - \theta_2\alpha_1 I_v - \theta_1\alpha_1 I_v y_1 + \theta_2\alpha_1 I_v y_1 + \theta_1\alpha_2 I_v r_1 y_2 - \alpha_2\theta_4 I_v r_1 y_2,\\
\frac{d\theta_2}{dt} &= \sigma\theta_2 - D_2 - \sigma\theta_3 + \theta_2\mu_h + \Omega\sigma\theta_3 - \Omega\sigma\theta_4 + \theta_2 r_2 y_3 - \theta_3 r_2 y_3,\\
\frac{d\theta_3}{dt} &= D_3 - \theta_3\mu_h - \theta_3 r_3 y_4 + \theta_4 r_3 y_4,\\
\frac{d\theta_4}{dt} &= \theta_4\mu_h - D_4 + \theta_4 r_4 y_5 + \beta_2\theta_5 r_6 y_7 S_v - \beta_2\theta_6 r_6 y_7 S_v,\\
\frac{d\theta_5}{dt} &= \theta_5\mu_v - D_5 + \theta_5 r_7 y_8 + \beta_2\theta_5 I_h r_6 y_7 - \beta_2\theta_6 I_h r_6 y_7 + \beta_1\theta_5 I_v r_5 y_6 - \beta_1\theta_6 I_v r_5 y_6,\\
\frac{d\theta_6}{dt} &= \theta_6\mu_v - D_6 + \theta_1\alpha_1 S_h - \theta_2\alpha_1 S_h + \theta_6 r_8 y_9 - \theta_1\alpha_1 y_1 S_h + \theta_2\alpha_1 y_1 S_h + \theta_1\alpha_2 r_1 y_2 S_h\\
&\quad - \alpha_2\theta_4\ r_1 y_2 S_h + \beta_1\theta_5 r_5 y_6 S_v - \beta_1\theta_6 r_5 y_6 S_v.
\end{aligned}$$

confirming adherence to the rule related to the constraints, where all $\theta_i(t) = 0$ for all $i = 1, 2, \ldots, 6$, then solution for the optimal control parameters $y^* = (y_1^*, y_2^*, y_3^*, y_4^*, y_5^*, y_6^*, y_7^*, y_8^*, y_9^*)$, is followed as.

$$\begin{aligned}
y_1^* &= \min\left\{\max\left\{0, \frac{(\theta_2-\theta_1)\alpha_1 I_v S_h}{B_1}\right\}, 1\right\}, \quad y_2^* = \min\left\{\max\left\{0, \frac{(\theta_1-\theta_4)\alpha_2 I_v r_1 S_h}{B_2}\right\}, 1\right\},\\
y_3^* &= \min\left\{\max\left\{0, \frac{(\theta_2-\theta_3)E_h r_2}{B_3}\right\}, 1\right\}, \quad y_4^* = \min\left\{\max\left\{0, \frac{(\theta_3-\theta_4)r_3 A_h r_2}{B_4}\right\}, 1\right\},\\
y_5^* &= \min\left\{\max\left\{0, \frac{(\theta_4)I_h r_4}{B_5}\right\}, 1\right\}, \quad y_6^* = \min\left\{\max\left\{0, \frac{(\theta_5-\theta_6)\beta_1 I_v r_5 S_v}{B_6}\right\}, 1\right\},\\
y_7^* &= \min\left\{\max\left\{0, \frac{(\theta_5-\theta_6)\beta_2 I_h r_6 S_v}{B_7}\right\}, 1\right\}, \quad y_8^* = \min\left\{\max\left\{0, \frac{(\theta_5)r_7 S_v}{B_8}\right\}, 1\right\},\\
y_9^* &= \min\left\{\max\left\{0, \frac{(\theta_6)I_v r_8}{B_9}\right\}, 1\right\}.
\end{aligned}$$

Proof Identifying the approach outlined in[39] it becomes feasible and practical to establish the constraints for achieving an optimal control purpose using Pontryagin's maximum principle. This study comprises assessing the following conditions:

$$\begin{aligned}
\frac{d\theta_1}{dt} &= -\frac{\partial H}{\partial S_h}, \quad \frac{d\theta_2}{dt} = -\frac{\partial H}{\partial E_h}, \quad \frac{d\theta_3}{dt} = -\frac{\partial H}{\partial A_h},\\
\frac{d\theta_4}{dt} &= -\frac{\partial H}{\partial I_h}, \quad \frac{d\theta_5}{dt} = -\frac{\partial H}{\partial S_v}, \quad \frac{d\theta_6}{dt} = -\frac{\partial H}{\partial I_v}.
\end{aligned}$$

There is an expression for the dynamics of the control factors, according to the defined transversion constraints where $\theta_i(t) = 0$ for all $i = 1, 2, \ldots, 6$.

$$\frac{\partial H}{\partial y_i} = 0, \quad \text{for } i = 1, 2, \ldots, 9.$$

It is confirmed that the control parameters' goal can be accomplished by limiting their values according to pivotal arguments.

$$y_i^* = \begin{cases} 0, & \text{if } \eta_i^* \le 0\\ \eta_i^*, & \text{if } 0 \le \eta_i^* \le 1\\ 1, & \text{if } \eta_i^* \ge 1 \end{cases}$$

where

Year	Cases	Year	Cases	Year	Cases	Year	Cases	Year	Cases
1996	149	2002	1200	2008	2544	2014	950	2020	202
1997	231	2003	2050	2009	2282	2015	831		
1998	231	2004	2733	2010	2116	2016	654		
1999	350	2005	2614	2011	1973	2017	531		
2000	517	2006	3376	2012	1474	2018	436		
2001	891	2007	3400	2013	1212	2019	309		

Table 1. Yearly reported cases from 1996 to 2020[34].

Parameter	Value	Description	Source
Λ	18118334.83	Rate of humans recruitment	[35,36]
μ_h	0.01350641	Natural death rate of humans	[35]
α_1	1.0×10^{-12}	Exposure rate from animal-human interaction	fitted
α_2	$[3.132 \times 10^{-12}, 3.5252 \times 10^{-12}]$	Infection rate from animal-human interaction	fitted
σ	[0.001, 0.1]	Rate of progression from exposure to infection	fitted
Ω	0.1	Asymptomatic case proportion in humans	fitted
Ψ	75000	Rate of animals recruitment	assumed
β_1	1.0×10^{-6}	Transmission rate among animals	fitted
β_2	1.0×10^{-7}	Transmission rate among humans-animals	fitted
μ_v	[0.1, 0.962]	Natural death rate of animals	fitted

Table 2. Parameter estimation for the rabies model.

$$
\begin{aligned}
\eta_1^* &= \frac{(\theta_2-\theta_1)\alpha_1 I_v S_h}{B_1},\\
\eta_2^* &= \frac{(\theta_1-\theta_4)\alpha_2 I_v r_1 S_h}{B_2},\\
\eta_3^* &= \frac{(\theta_2-\theta_3)E_h r_2}{B_3},\\
\eta_4^* &= \frac{(\theta_3-\theta_4)r_3 A_h r_2}{B_4},\\
\eta_5^* &= \frac{\theta_4 I_h r_4}{B_5},\\
\eta_6^* &= \frac{(\theta_2-\theta_1)\alpha_1 I_v S_h}{B_1},\\
\eta_7^* &= \frac{(\theta_2-\theta_1)\alpha_1 I_v S_h}{B_1},\\
\eta_8^* &= \frac{(\theta_2-\theta_1)\alpha_1 I_v S_h}{B_1},\\
\eta_9^* &= \frac{(\theta_2-\theta_1)\alpha_1 I_v S_h}{B_1}.
\end{aligned}
$$

The proof is now completed. □

Analyzing the efficacy of the employed techniques is necessary to achieve the goal. Using the parameter values listed in Table 1 and an initial reproduction number of $R_0 = 3.31211$, the task has a strategic time of 25 years. The distribution of auspicious weights is as follows: $D_1 = 1, D_2 = 5, D_3 = 10, D_4 = 15, D_5 = 20, D_6 = 25$. Further, $B_1 = 3, B_2 = 6, B_3 = 9, B_4 = 12, B_5 = 15, B_6 = 18, B_7 = 21, B_8 = 24, B_9 = 27$. The initial conditions are set as: $S_h(0) = 1228298836,\ E_h(0) = 1000,\ A_h(0) = 700,\ I_h(0) = 149,\ S_v(0) = 600000,\ I_v(0) = 15000$. The primary objective is to reduce the number of fatalities and enhance recuperation by implementing comprehensive safety measures elucidated with visual representations.

Effectiveness of control strategies

Figure (6) signifies the efficacy of controls applied to the model to minimize the rabies spread.

- The susceptible human population grows due to preventive measures taken to stop them from moving into other zones, as seen in Figure (6a).

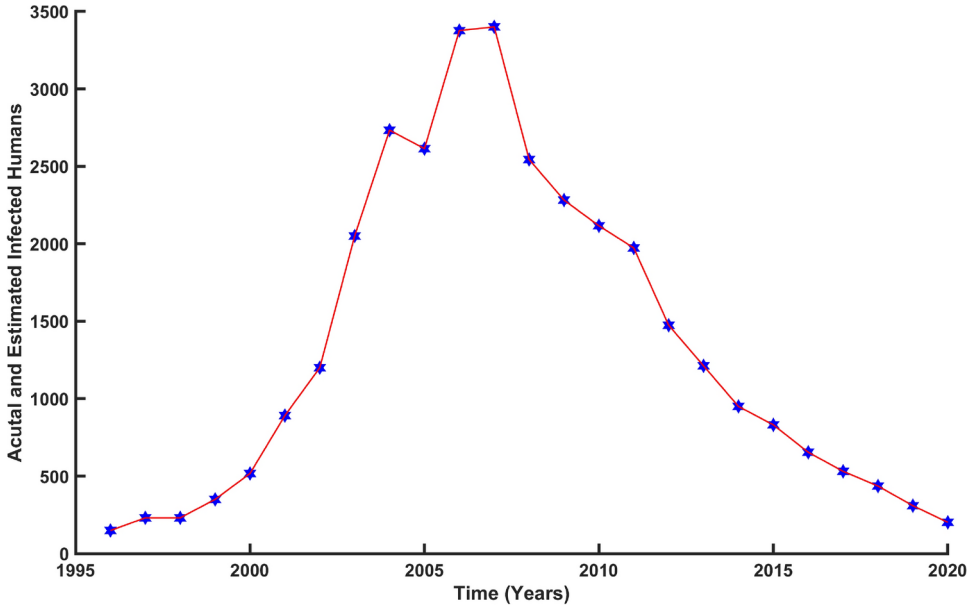

Fig. 3. Comparison of estimated rabies cases (depicted by the red line) and actual rabies cases (depicted by stars).

Parameter	Description	Sensitivity Index	Sign
Λ	Rate of humans recruitment	$[4.10562 \times 10^{-3}, 0.199649]$	+ve
μ_h	Natural death rate of humans	$[-0.399878, -8.21964 \times 10^{-3}]$	-ve
α_1	Exposure rate from animal-human interaction.	$[9.01659 \times 10^{-6}, 4.86792 \times 10^{-3}]$	+ve
α_2	Infection rate from animal-human interaction	$[4.0966 \times 10^{-3}, 0.194782]$	+ve
σ	Rate of progression from exposure to infection	$[8.39503 \times 10^{-6}, 5.79246 \times 10^{-4}]$	+ve
Ω	Asymptomatic case proportion in humans	$[9.01659 \times 10^{-6}, 4.86792 \times 10^{-3}]$	+ve
Ψ	Rate of animals recruitment	[0.800351, 0.995894]	+ve
β_1	Transmission rate among animals	[0.600701, 0.991789]	+ve
β_2	Transmission rate among human-animal	$4.10562 \times 10^{-3}, 0.199649]$	+ve
μ_v	Natural death rate of animals	$[-1.99179, -1.6007]$	-ve

Table 3. Sensitivity indices.

- The results shown in Figure (6b) demonstrate that after control implementation, the number of exposed humans decreased, indicating that people are not moving into the exposed class.
- Figure (6c) illuminates that the asymptotic human population gradually decreased after applying control measures.
- The population of infected humans eventually begins to decline, as seen in Figure (6d), demonstrating the effectiveness of all measures in halting the spread of rabies.
- As can be shown in Figure (6e), the susceptible animal population moves into other zones or is eliminated when controls are used.
- Following control measures, the infected animal population significantly declined, as shown in Figure (6f).

Percentage effectiveness
The effectiveness of each control is shown over time in Figure (7), which is explained below.

- Control y_1 initiates with an initial effectiveness of 78%, which then decreases with the passage of time.
- Control y_2 starts with 100% efficacy when applied, and it starts decreasing and shows stability for 16 years.
- Control y_3 exhibits an initial efficacy of 83%, then followed by significant stability with an efficacy 75% till 24 years.
- Control y_4 initiates with an initial effectiveness of 11%, gradually it decreases and becomes ineffective after one year.
- Control y_5 initially achieves 89% efficacy, which starts decreasing till the end of the year. It remains effective with the stability of 11% years, then its effectiveness diminishes.

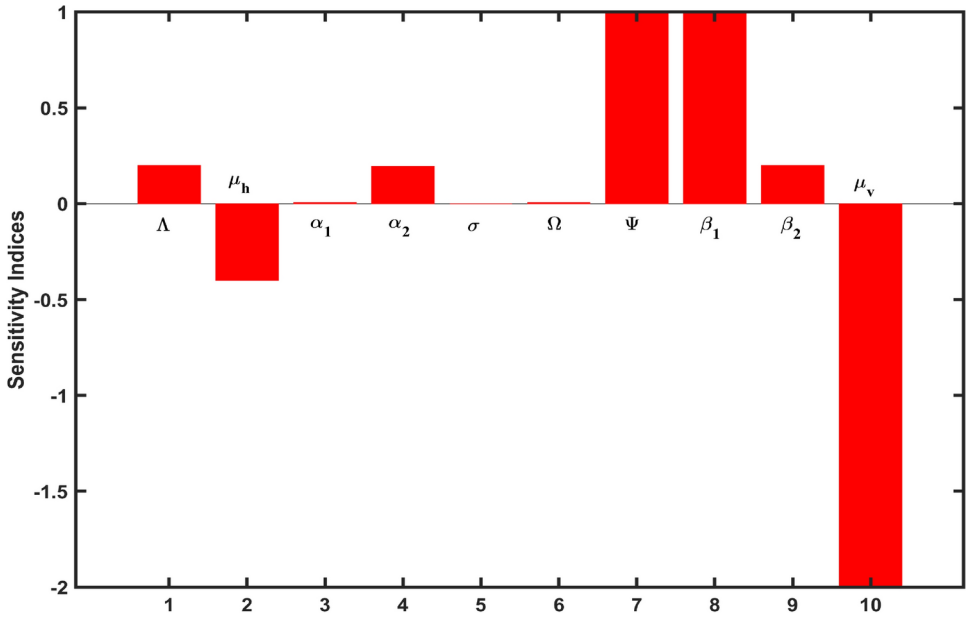

Fig. 4. Visualization of sensitivity indices.

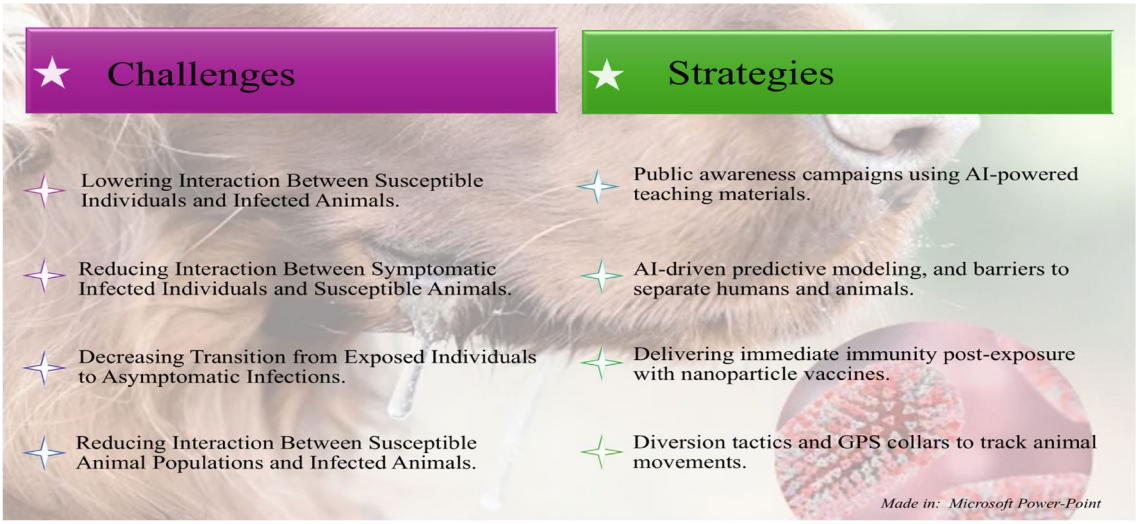

Fig. 5. Challenges and Strategies.

- Control y_6 gradually loses efficacy after one year of application, which was 18% at first.
- Control y_7 has an efficacy of 19% at the time of implementation, but after a year, it starts to lose its effectiveness.
- Control y_8 exhibits 48% initial efficacy which slightly decreases, increases again after 7 years, and ultimately stabilizes at 76% efficacy for the next 24 years.
- Control y_9 starts with a 5% efficacy when applied, and within one year, it loses its effectiveness.

Conclusion

This study employs a novel methodology known as Sans Recuperation for the mathematical formulation, statistical analysis, and strategic examination to comprehend and control rabies disease. This innovative approach aims to enhance the understanding of dissemination and develop efficient eradication strategies.

The dynamics of rabies spread are examined using the Rabies sans recuperation model, and the model's accuracy is confirmed by calibrating real-world data on rabies. Moreover, locally and globally, the stability of endemic and rabies-free states is examined. Estimating factors and calculating the basic reproduction rate are also conducted. Sensitivity analysis is carried out to measure and assess how critical parameters influence rabies propagation.

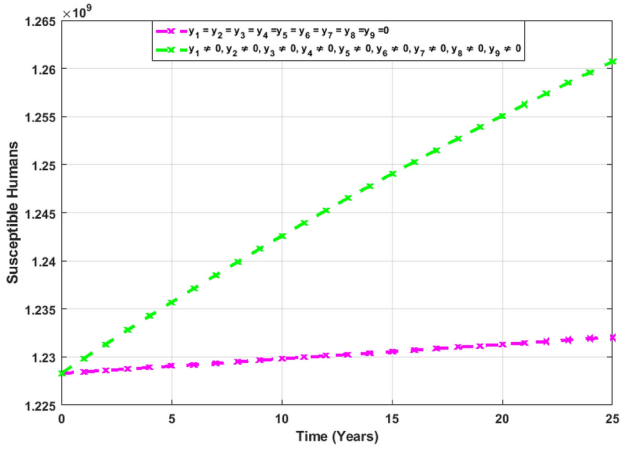

(a)

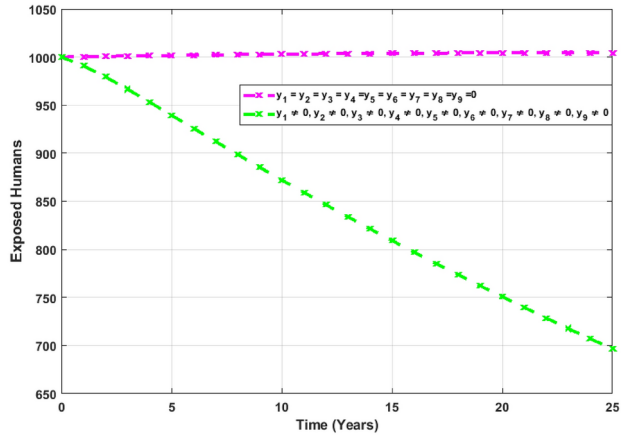

(b)

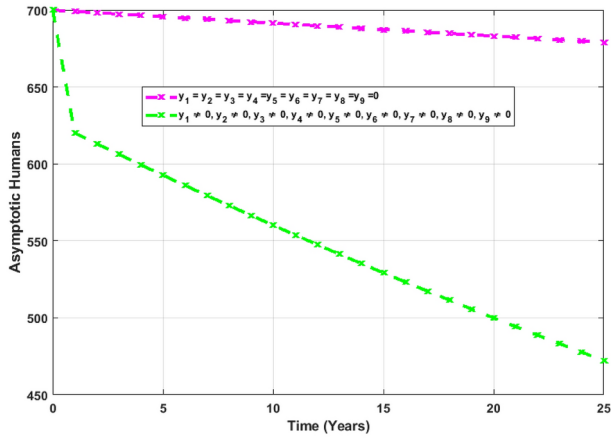

(c)

Fig. 6. Use of controls with the estimated values of parameters.

Further, a controlled model is developed based on sensitivity analysis. Several approaches have been suggested, and their effectiveness is envisioned, emphasizing the uniqueness of this study in abolishing rabies. Most importantly, based on the control profile, strategies can be developed while keeping an eye on the efficacy of each control. The main objective is to develop early diagnosis, cure, and remediation endeavors, firming up the ability to react onsets successfully to decrease the neurological impacts and fatalities linked with rabies disease.

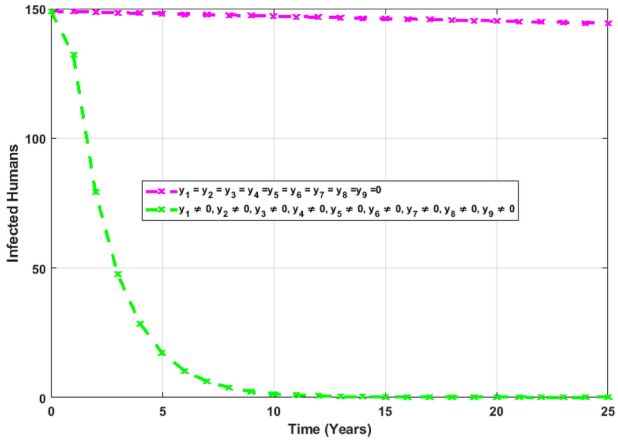

(d)

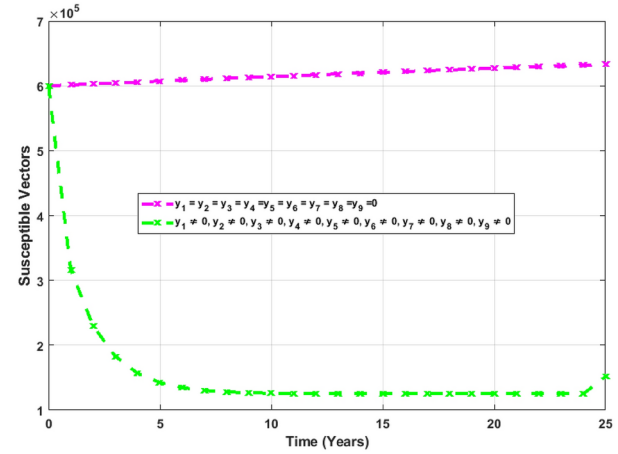

(e)

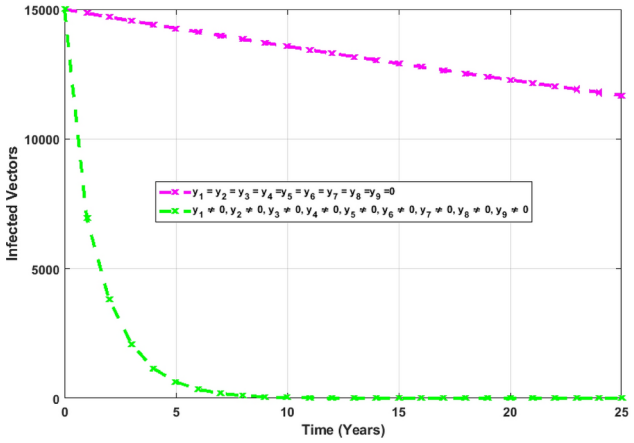

(f)

Figure 6. (continued)

Future research in this field explores leveraging nanotechnology and artificial intelligence to integrate more inclusive epidemiological data and enhance data collection and scrutiny systems. The focus is on developing cost-effective strategies to mitigate the spread of rabies and address disabilities resulting from the disease.

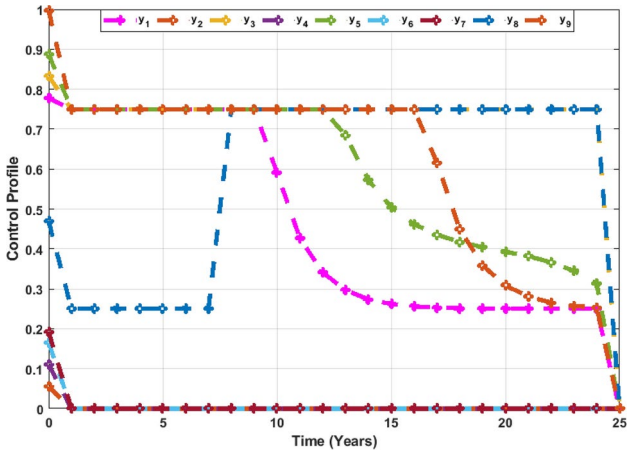

Fig. 7. Effectiveness of all controls.

Data availability

The data used to support the findings of this study is included within the article.

Received: 11 November 2024; Accepted: 2 May 2025
Published online: 19 May 2025

References

1. Liu, C. H. History of rabies control in Taiwan and China. *Epidemiology Bulletin* **29**, 44–52 (2013).
2. Meissner, E. G. et al. Immuno suppressed the bone marrow did not reconstitute, and 35 days after. *Emerging Infectious Diseases* **18**, 1155 (2012).
3. Guedri, K. et al. Rabies-related brain disorders: Transmission dynamics and epidemic management via educational campaigns and application of nanotechnology. *The European Physical Journal Plus* **139**, 49 (2024).
4. Yu, Y. X. *Rabies and rabies vaccine* 10–20 (Chinese Medicine Technology Press, Beijing, 2001).
5. Jackson, A. C. & Human Rabies: A,. Update. *Current Infectious Disease Reports* **18**(2016), 1–6 (2016).
6. Baer, G. M., The History of Rabies. *Academic Press*. 1-22 (2007).
7. Garg, S. R. Rabies in Man and Animals. *Springer*. 14844 (2014).
8. Fekadu, M. Canine rabies. *Onderstepoort. J. Vet. Res.* **60**, 421–427 (1993).
9. Singh, R. et al. Rabies-epidemiology, pathogenesis, public health concerns and advances in diagnosis and control: a comprehensive review. *Vet. Q.* **37**, 212–251 (2017).
10. Hampson, K. et al. Estimating the global burden of endemic canine rabies. *PLoS Negl. Trop. Dis.* **9**, e0003709 (2015).
11. Hou, Q., Jin, Z. & Ruan, S. Dynamics of rabies epidemics and the impact of control efforts in Guangdong Province, China. *J. Theor. Biol.* **300**, 39–47 (2012).
12. Dreesen, D. W. A global review of rabies vaccines for human use. *Vaccine* **15**, S2–S6 (1997).
13. Organization, W. H. WHO Expert Consultation on Rabies Second Report. *World Health Organization*, **982**(2013).
14. Kumar, A., Bhatt, S., Kumar, A. & Rana, T. *Canine Rabies: An Epidemiological Significance, Pathogenesis, Diagnosis* 101992 (Prevention and Public Health Issues. Comparative Immunology, Microbiology and Infectious Diseases, 2023).
15. Bannazadeh Baghi, H., Alinezhad, F., Kuzmin, I. & Rupprecht, C. E. A Perspective on Rabies in the Middle East-Beyond Neglect. *Vet. Sci.* **5**, 67 (2018).
16. Swinkels, H. M., Koury, R., Warrington, S. J., Rabies. *National Center of Biotechnology Information*, https://www.ncbi.nlm.nih.gov/books/NBK448076/#:~:text=Rabies%20is%20one%20of%20the,animal%2C%20many%20would%20commit%20suicide, accessed on April (2025).
17. Hemachudha, T. et al. Human Rabies: Neuropathogenesis, diagnosis, and management. *The Lancet Neurology* **12**, 498–513 (2013).
18. Klein, R. S. Rabies. https://www.msdmanuals.com/home/brain,-spinal-cord,-and-nerve-disorders/brain-infections/rabies, accessed on April 2025.
19. Hamam, H. et al. Deciphering the enigma of lassa virus transmission dynamics and strategies for effective epidemic control through awareness campaigns and rodenticides. *Sci. Rep.* **14**, 18079 (2024).
20. Ramzan, Y., Awan, A. U., Ozair, M., Hussain, T. & Mahat, R. Innovative strategies for lassa fever epidemic control: a groundbreaking study. *AIMS Mathematics* **8**, 30790–30812 (2023).
21. Guedri, K., Ramzan, Y., Awan, A. U., Fadhl, B. M. & Oreijah, M. Modeling Transmission Patterns and Optimal Control through Nanotechnology: A Case Study of Malaria Causing Brain Disabilities. *Journal of Disability Research* **3**, 20230061 (2023).
22. Zainab, M. et al. A fractional-operator approach for unraveling rabies disease dynamics in animal population. *Alexandria Engineering Journal* **124**, 540–549 (2025).
23. Charles, M., Mfinanga, S. G., Lyakurwa, G. A., Torres, D. F. & Masanja, V. G. Parameters Estimation and Uncertainty Assessment in the Transmission Dynamics of Rabies in Humans and Dogs. *Chaos. Solitons. Fractals.* **189**, 115633 (2024).
24. Panjeti, V. G. & Real, L. A. Mathematical Models for Rabies. *Adv. Virus. Res.* **79**, 377–395 (2011).
25. Ruan, S. Modeling the Transmission Dynamics and Control of Rabies in China. *Math. Biosci.* **286**, 65–93 (2017).
26. Lu, W. G. et al. Epidemiological and Numerical Simulation of Rabies Spreading from Canines to Various Human Populations in Mainland China. *PLoS Negl. Trop. Dis.* **15**, e0009527 (2021).
27. Zainab, M. et al. Study of Fractional Order Rabies Transmission Model via Atangana-Baleanu Derivative. *Sci. Rep.* **14**, 25875 (2024).
28. Hussain, T., Aslam, A., Ozair, M., Tasneem, F. & Gómez-Aguilar, J. F. Dynamical Aspects of Pine Wilt Disease and Control Measures. *Chaos. Solitons. Fractals.* **145**, 110764 (2021).
29. Van den Driessche, P. & Watmough, J. Reproduction Numbers and Sub-Threshold Endemic Equilibria for Compartmental Models of Disease Transmission. *Math. Biosci.* **180**, 29–48 (2002).

30. Collins, O. C. & Govinder, K. S. Stability Analysis and Optimal Vaccination of a Waterborne Disease Model with Multiple Water Sources. *Natural Resource Modeling* **29**, 426–447 (2016).
31. Patil, A. Routh-Hurwitz Criterion for Stability: An Overview and its Implementation on Characteristic Equation Vectors using MATLAB. *Emerging Technologies in Data Mining and Information Security: Proceedings of IEMIS* **2020**(1), 319–329 (2021).
32. Castillo-Chavez, C., Blower, S., van den Driessche, P., Kirschner, D., & Yakubu, A. A., Mathematical approaches for emerging and reemerging infectious diseases: models, methods, and theory. *Springer Science & Business Media*, (2002).
33. Walker, J. A. Dynamical Systems and Evolution Equations: Theory and Applications. *Springer Science Business Media*, **20**(2013).
34. Shen, T., Welburn, S. C., Sun, L. & Yang, G. J. Progress Towards Dog-Mediated Rabies Elimination in PR China: A Scoping Review. *Infect. Dis. Poverty.* **12**, 30 (2023).
35. Life Expectancy. *Macrotrends*, https://www.macrotrends.net/countries/CHN/china/life-expectancy, accessed on April 2025.
36. Population. *Macrotrends*, https://www.macrotrends.net/countries/CHN/china/population, accessed on April 2025.
37. Chitnis, N., Hyman, J. M. & Cushing, J. M. Determining Important Parameters in the Spread of Malaria through the Sensitivity Analysis of a Mathematical Model. *Bull. Math. Biol.* **70**, 1272–1296 (2008).
38. Pontryagin, L. S. Mathematical Theory of Optimal Processes. *CRC Press*, **4**(1987).
39. Fleming, W. H., Rishel, R. W. Deterministic and Stochastic Optimal Control. *Springer Science Business Media*, **1**, (2012). .
40. Ramzan, Y. et al. A Mathematical Lens on the Zoonotic Transmission of Lassa Virus Infections Leading to Disabilities in Severe Cases. *Math. Comput. Appl.* **29**, 102 (2024).

Acknowledgements
The authors extend their appreciation to the King Salman center For Disability Research for funding this work through Research Group no KSRG-2024-184.

Author contributions
Y.R.: Conceptualization; Formal analysis; Writing original draft preparation; Revision. B.M.F.: Methodology; Resources; Data Curation; Revision. S.N.: Investigation; Validation; Revision. A.U.A: Formal analysis; Visualization; Review and editing; supervision. K.G.: Software; Resources; Investigation; Revision.

Funding
The authors extend their appreciation to the King Salman center For Disability Research for funding this work through Research Group no KSRG-2024-184.

Declarations

Competing interest
The authors declare no competing interests.

Declaration of generative AI in scientific writing
All authors declare to no use of AI-assisted technologies in article writing process.

Ethical approval
All the authors declare that our manuscript fulfills all ethical research standards.

Additional information
Correspondence and requests for materials should be addressed to S.N.